# Defense Technical Information Center Compilation Part Notice

# ADP012648

TITLE: High-Performance InAs/GaAs Quantum Dots Infrared Photodetector With/Without Al[0.2]Ga[0.8]As Blocking Layers

DISTRIBUTION: Approved for public release, distribution unlimited

## This paper is part of the following report:

TITLE: Progress in Semiconductor Materials for Optoelectronic Applications Symposium held in Boston, Massachusetts on November 26-29, 2001.

To order the complete compilation report, use: ADA405047



The following component part numbers comprise the compilation report:
ADP012585 thru ADP012685

Mat. Res. Soc. Symp. Proc. Vol. 692 © 2002 Materials Research Society 

# High-Performance InAs/GaAs Quantum Dots Infrared Photodetector With/Without $Al_{0.2}Ga_{0.8}As$ Blocking Layers

Zhengmao Ye, Joe C. Campbell
Microelectronics Research Center, The University of Texas at Austin,
10,100 Burnet Rd., Bldg. 160, Austin, TX 78758, U.S.A.

Zhonghui Chen, O. Baklenov, E. T. Kim, I. Mukhametzhanov, J. Tie, and A. Madhukar,
Departments of Materials Science and Physics University of Southern California,
Los Angeles, CA 90089-0241, U.S.A.

## ABSTRACT

InAs/AlGaAs quantum dot infrared photodetectors based on bound-to-bound intraband transitions in undoped InAs quantum dots are reported. AlGaAs blocking layers were employed to achieve low dark current. The photoresponse peaked at 6.2 μm. At 77 K and –0.7 V bias the responsivity was 14 mA/W and the detectivtiy, D*, was $10^{10}$ $cmHz^{1/2}/W$.

## INTRODUCTION

Mid and far-infrared (3-20 μm) detection is a key technology for numerous commercial, military and space applications, e.g., night vision, thermal imaging, chemical analysis, non-destructive detecting, remote sensing, and missile guidance and defense. Due to the long carrier capture and relaxation times, quantum dot infrared photodetectors (QDIPs) have the potential for lower dark current and higher photoresponse than quantum well infrared photodetectors (QWIPs). Most importantly, the three-dimensional confinement of electrons in the quantum dots permits QDIPs to operate in the normal incidence mode, unlike QWIPs which are not sensitive to radiation that is incident perpendicular to the quantum wells [1]. To date, there have been several papers on InAs/GaAs, InGaAs/GaAs and InGaAs/InGaP QDIPs [2]-[10]. Most of the devices employed a doped active region, which resulted in high dark current. In this paper, we report an InAs/GaAs QDIP with unintentionally doped active region and AlGaAs barrier layers (sample A). The AlGaAs layers act as a blocking layer [6]-[10] for dark current, as first demonstrated in Ref. 6. The devices reported here have demonstrated low dark current, low noise, and high detectivity.

## DEVICE STRUCTURES AND FABRICATIONS

The InAs QDIPs studied in this work belong to the class of n-i-n structure QDIPs (Figure 1) under examination by us [6][7]. The samples were grown on semi-insulating GaAs (001) substrates by solid-source molecular beam epitaxy. Five layers of 3 monolayer (ML) InAs quantum dots were inserted between highly Si-doped top and bottom GaAs contact layers. The punctuated island growth technique was used to grow the quantum dots [11]. The GaAs spacer layers between the contact layers and the nearest quantum dot layer had a thickness of 219 ~ 239 ML. 30 ML GaAs regions were used as the quantum dot cap layers. In order to reduce the dark current, four pairs of AlAs/GaAs (1 ML/ 4 ML) were introduced below the quantum dot layers and on the top of the GaAs cap layers (sample A). A similar QDIP without blocking layers

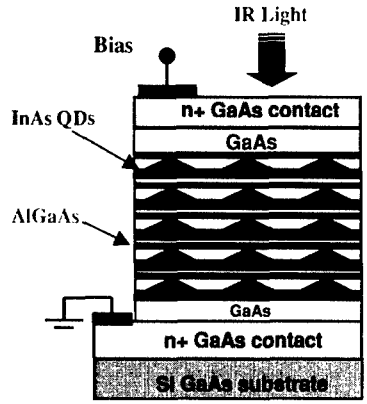


**Fig. 1** Schematic of InAs/GaAs QDIP structure (e.g. with AlGaAs blocking layers).

(sample B) was also used. The sizes of the pyramidal-shaped quantum dots of sample B and A were estimated with atomic force microscopy (AFM) and a cross-sectional transmission electron microscope (XTEM): the height was 74±16 Å and 59±17 Å, respectively. Both dots have a base width of 210 Å. The dot densities of sample B and A was 673±60 /$\mu m^2$ and 625±40 /$\mu m^2$, respectively.

Device fabrication followed standard procedure: photolithography, wet chemical etching, metal deposition and lift-off, and rapid thermal annealing. Mesas having a diameter of 250 μm and a height of ~1.4 μm were defined with an etch of $H_3PO_4$ : $H_2O_2$ : $H_2O$ (8:1:1). A 50 μm-diameter top contact and the bottom contact were formed by evaporation and liftoff of Au/Ni/AuGe. The contacts were then annealed at 430 °C for 20 seconds. In the following discussion, "positive" bias means that a positive voltage was applied to the top contact.

## DISCUSSION

### Spectral response

The normal-incidence spectral response was measured with a Nicolet Magna-IR 570 Fourier transform infrared (FTIR) spectrometer and a SRS 570 low-noise current preamplifier. Figure 2 shows the spectral response of sample A at 0.8 V bias and at temperatures of 63 K, 77 K and 100 K. The intraband photoresponse peaks occurred at 6.2 μm for all three spectra. The full width half maximum (FWHM) of the spectrum, $\Delta\lambda$, was ~ 0.4 μm, from which it follows that $\Delta\lambda/\lambda$=7.5%. The narrow spectral width is consistent with our previous results [7][12]. These results indicate that the electron transitions are intraband transitions from a lower bound state to a higher bound state [12]. The observed spectral width reflects the uniformity of the size of the quantum dots. The QDIP exhibits the highest photoresponse at 77 K. This can be explained as follows: As the temperature increases, more electrons occupy the lower states of the quantum dots. As long as there are unoccupied excited states available, the electrons in the lower states can participate in photon induced intraband transitions. However, further increase in the number

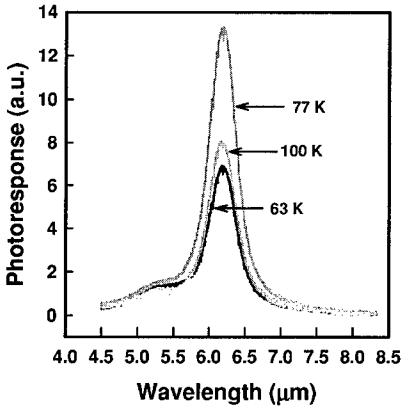


**Fig.2** Normal-incident photoresponse of the QDIP sample A at the bias of 0.8 V and temperature of 63 K, 77K and 100K.

of electrons in the quantum dots, which results from the increase in dark current at higher temperature, will cause a decrease in the number of unoccupied excited states and, consequently, a decrease in the photoresponse. Additionally, a decrease in photo-excited electron lifetime at higher temperature can result in a decrease in the photoresponse, too.

Responsivity

The absolute spectral responsivity was calibrated with a blackbody source (T = 995 K). Since the blackbody spectrum included near infrared radiation, which could result in interband transitions, in addition to mid- and long-wavelength photons, optical filters were placed next to the aperture of the blackbody to block radiation with wavelength less than 3.5 μm. Figure 3 shows the peak spectral responsivity versus bias of at temperatures of 77 K, 100 K, and 120 K. With increase in positive bias, the responsivity increased from 0.33 mA/W at 0.1V to 280 mA/W at 1.7V. For negative bias, the responsivity increased near four orders of magnitude from $5.2\times10^{-2}$ mA/W at zero bias to 418 mA/W at –1.6 V. Negative differential responsivity, which was shown in sample B, was not observed within the bias range from –1.6 V to 1.7 V. The different responsivity curves for the positive and negative bias are attributed to the asymmetric shape of the quantum dots along the growth direction and the wetting layers beneath the quantum dots. Consequently, electrons in the quantum dots experience different barrier heights depending on whether transport is toward the top or bottom contacts. Due to the introduction of the $Al_{0.2}Ga_{0.8}As$ blocking layers, the responsivity of sample A is lower than that of sample B.

Dark current

Dark current density versus voltage characteristic of sample A is shown in Fig. 4 for temperature in the range from 60 K to 296 K. The structural asymmetry of the quantum dots also

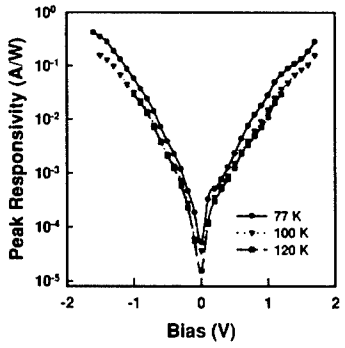


**Fig. 3** Peak responsivity of sample A at 77 K, 100K, and 120K.

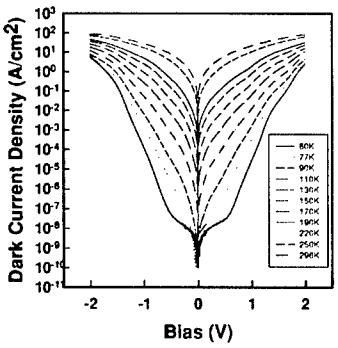


**Fig. 4** Dark current density of sample A at temperature ranging from 60 K to 296K.

results in asymmetrical dark current density for positive and negative bias. At low bias, the increase in dark current density is due to the fact that as the bias increases, more electrons occupy the quantum dots, which results in an increase in the average sheet electron density. When a large fraction of the quantum dots states are occupied, further increase in bias does not significantly alter the sheet electron density. This causes a lowering of the energy barrier for injected electrons at the contact layers, which results in the nearly exponential increase of the dark current. At 0.7 V bias, the dark current density was $2.5\times10^{-7}$ A/cm$^2$ at 60 K. With increasing temperature, it increased over seven orders of magnitude to 11.1 A/cm$^2$ at room temperature. Similarly, at –0.7 V bias, there was an increase of over eight orders of magnitude from $1.6\times10^{-7}$ A/cm$^2$ at 60 K to 14.4 A/cm$^2$ at 296 K. Compared to the similar structure without the $Al_{0.2}Ga_{0.8}As$ blocking layers, sample B, the dark current has been suppressed by over three orders of magnitude. For bias < 0.7 V and T > 100 K, the dark current increased exponentially with temperature, which suggests that in this temperature range the dark current originates from thermionic emission. The calculated activation energy was 196 meV at zero bias, which was close to the energy corresponding to the cutoff wavelength (193 meV) of the sample. For temperature lower than 100 K, sequential resonant tunneling and phonon assisted tunneling are probably the dominant components of the dark current.

Noise current

The noise current, $i_n$, was characterized with low noise current preamplifiers and a SRS 760 FFT spectrum analyzer. For $|V_B| > 0.6$ V, the noise current was measured with a SRS current preamplifier. However, below 0.6 V, the photodetector noise current of sample A was below the noise floor of the instrument. Near zero bias, a very low noise current preamplifier with high gain was used. However, restricted by the input power limitation of this current preamplifier, in the bias range from 0.1 V to 0.5 V and –0.5 V to –0.1 V, the noise current was interpolated.

Figure 4 shows the noise current of a 250 μm-diameter device at 77 K and 100 K. The calculated thermal noise current, $I_{th}$, at 77 K is also shown. The thermal noise current can be expressed as,

$$I_{th} = \sqrt{\frac{4\ kT}{R}} \quad (1)$$

where k is Boltzmann's constant, T is the absolute temperature, and R is the differential resistance of the device, which was extracted from the dark current. At $V_B$ = -0.7 V, the calculated thermal noise current ($3.2\times10^{-14}$ A/Hz$^{1/2}$) was very close the measured noise current ($2.9\times10^{-14}$ A/Hz$^{1/2}$), which indicates that thermal noise is significant in the low bias region. As the bias was increased, the noise current increased much faster than thermal noise. The noise current was greatly suppressed near three orders of magnitude by introducing $Al_{0.2}Ga_{0.8}As$ blocking layers.

Detectivity

The detectivity is given by

$$D^* = \frac{R\sqrt{A\cdot\Delta f}}{i_n} \quad (2)$$

where A is the device area, R is the responsivity, $i_n$ is the noise current, and $\Delta f$ is the bandwidth. Figure 6 shows the peak detectivity versus bias at 77 K and 100 K. The best performance was achieved at 77 K and –0.7 V where the peak detectivity was $10^{10}$ cmHz$^{1/2}$/W. The corresponding responsivity was 14 mA/W. With increase in temperature to 100 K, the peak detectivity dropped to $1.1\times10^{9}$ cmHz$^{1/2}$/W at 0.5 V, due to the decrease in responsivity and increase in noise current. The peak detectivity of sample B is $1.5\times10^{9}$ cmHz$^{1/2}$/W at 77 K. Therefore, the detectivity was enhanced over 6 times by using $Al_{0.2}Ga_{0.8}As$ blocking layers.

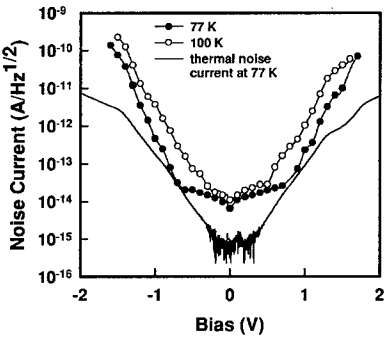


**Fig. 5** Measured noise current (dots) of sample A at 77 K and 100 K, and calculated thermal noise current at 77K.

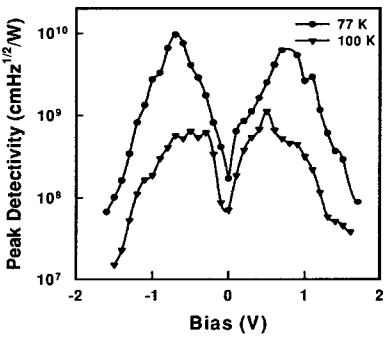


**Fig. 6** Peak detectivity of sample A at 77 K and 100 K.

## CONCULSIONS

In conclusion, we have demonstrated QDIPs based on bound-to-bound intraband transitions. These QDIPs were sensitive to normal-incident infrared radiation and exhibited low dark current with $D^*=9.6\times10^9$ cmHz$^{1/2}$/W and R= 14 mA/W at –0.7 V bias and 77 K. In contrast, the QDIPs with the same structure, except with GaAs barrier layer, exhibited $D^*=1.5\times10^9$ cmHz$^{1/2}$/W at 77 K.

## ACKNOWLEDGEMENTS

The authors would like to thank Dr. Jeff Beck of the DRS for help with calibration of responsivity and valuable discussions. This work was supported by AFOSR under the MURI program.

## REFERENCE

[1] V. Ryzhii, Sci. Technol. 11, 759 (1996)
[2] D. Pan, E. Towe, and S. Kennerly, Appl. Phys. Lett. 75, 2719 (1999).
[3] S. Kim, H. Mohseni, M. Erdtmann, E. Michel, C. Jelen, and M. Razeghi, Appl. Phys. Lett. 73, 963 (1998).
[4] J. Phillips, Pallab Bhattacharya, S.w. Kennerly, D.W. Beekman and M. Dutta, IEEE J. Quant. Electron. 35, 936 (1999).
[5] Jong-Wook Kim, Jae-Eung Oh, Seomg-Chul Hong, Chung-Hoon Park and Tae-Kyung Yoo, IEEE Electron Device Letter, 21, No. 7, 329 (2000).
[6] O. Baklenov, Z.H. Chen, E.T. Kim, I. Mukhametzhanov, A. Madhukar, F. Ma, Z. Ye, B. Yang, and J. Campbell, the 58th IEEE Device Research Conference, (Denver, Colorado, June 19-21, 2000), p171; Z.H. Chen, O. Baklenov, E.T. Kim, I. Mukhametzhanov, J. Tie, A. Madhukar, Z. Ye, and J. Campbell, Proceeding of QWIP2000 Workshop, Dana Point, CA, July 2000, Infrared Physics & Technology, 42, 479 (2001)
[7] Z.H. Chen, O. Baklenov, E. T. Kim, I. Mukhametzhanov, J. Tie, A. Madhukar, Z. Ye and J. C. Campbell, J. Appl. Phys. 89, 4558 (2001).
[8] S. Y. Wang, S. D. Lin, H. W. Wu, and C. P. Lee, Appl. Phys. Lett., 78, 1023 (2001).
[9] Shih-Yen Lin, Yau-Ren Tsai, and Si-chen Lee, Appl. Phys. Lett., 78, 2784 (2001).
[10] A.D. Stiff, S. Krishna, P. Bhattacharya, and S. Kennerly, Appl. Phys. Lett. 79, 421 (2001)
[11] I. Mukhametzhanov, Z. Wei, Rheitz, and A. Madhukar, Appl. Phys. Lett., 75, 85 (1999).
[12] I. Mukhametzhanov, Z.H. Chen, O. Baklenov, E.T. Kim, and A. Madhukar, Phys. Status Solidi (b) 224, 697 (2001)